Primary Cilium in Neural Crest Cells Crucial for Anterior Segment Development and Corneal Avascularity

Seungwoon Seo,[1,2] Seong Keun Sonn,[1] Hyae Yon Kweon,[1] Jing Jin,[1] Tsutomu Kume,[3] Je Yeong Ko,[4] Jong Hoon Park,[4] and Goo Taeg Oh[1,2]

[1]Heart-Immune-Brain Network Research Center, Department of Life Science, Ewha Womans University, Seoul, Republic of Korea
[2]Imvastech Inc., Seoul, Republic of Korea
[3]Feinberg Cardiovascular and Renal Research Institute, Northwestern University School of Medicine, Chicago, Illinois, United States
[4]Department of Biological Science, Sookmyung Women's University, Seoul, Republic of Korea

Correspondence: Jong Hoon Park, Department of Biological Science, Sookmyung Women's University, Seoul 04310, Republic of Korea; parkjh@sookmyung.ac.kr.
Goo Taeg Oh, Heart-Immune-Brain Network Research Center, Department of Life Science, 52 Ewhayeodaegil, 305 Science Building C, Ewha Womans University, Seoul 03760, Republic of Korea; gootaeg@ewha.ac.kr.

SS and SKS contributed equally to this work and are co-first authors.

Received: December 15, 2023
Accepted: February 26, 2024
Published: March 22, 2024

Citation: Seo S, Sonn SK, Kweon HY, et al. Primary cilium in neural crest cells crucial for anterior segment development and corneal avascularity. *Invest Ophthalmol Vis Sci.* 2024;65(3):30. https://doi.org/10.1167/iovs.65.3.30

Purpose. Intraflagellar transport 46 (IFT46) is an integral subunit of the IFT-B complex, playing a key role in the assembly and maintenance of primary cilia responsible for transducing signaling pathways. Despite its predominant expression in the basal body of cilia, the precise role of *Ift46* in ocular development remains undetermined. This study aimed to elucidate the impact of neural crest (NC)-specific deletion of *Ift46* on ocular development.

Methods. NC-specific conditional knockout mice for *Ift46* (NC-*Ift46*$^{F/F}$) were generated by crossing *Ift46*^{F} mice with *Wnt1-Cre2* mice, enabling the specific deletion of *Ift46* in NC-derived cells (NCCs). Sonic Hedgehog (Shh) and Notch signaling activities in NC-*Ift46*$^{F/F}$ mice were evaluated using *Gli1*^{lacZ} *and CBF:H2B-Venus* reporter mice, respectively. Cell fate mapping was conducted using *ROSA*^{mTmG} reporter mice.

Results. The deletion of *Ift46* in NCCs resulted in a spectrum of ocular abnormalities, including thickened corneal stroma, hypoplasia of the anterior chamber, irregular iris morphology, and corneal neovascularization. Notably, this deletion led to reduced Shh signal activity in the periocular mesenchyme, sustained expression of key transcription factors Foxc1, Foxc2 and Pitx2, along with persistent cell proliferation. Additionally, it induced increased Notch signaling activity and the development of ectopic neovascularization within the corneal stroma.

Conclusions. The absence of primary cilia due to *Ift46* deficiency in NCCs is associated with anterior segment dysgenesis (ASD) and corneal neovascularization, suggesting a potential link to Axenfeld-Rieger syndrome, a disorder characterized by ASD. This underscores the pivotal role of primary cilia in ensuring proper anterior segment development and maintaining an avascular cornea.

Keywords: Ift46, primary cilium, ASD, cornea, neovascularization, neural crest-derived cells

Anterior segment dysgenesis (ASD) encompasses various congenital disorders disrupting the proper functioning of the eye's anterior segment structures, leading to corneal opacification, corneal thickening, lens-corneal attachment, and iridocorneal adhesions.[1,2] Axenfeld-Rieger syndrome (ARS), a rare congenital condition primarily affecting the anterior segment of the eye, is associated with autosomal dominant mutations in *FOXC1* and *PITX2*, governing neural crest-derived cells' (NCCs) contributions to ocular development.[3–5] During this process, NCCs migrate into the periocular mesenchyme (POM), crucial for shaping the anterior segment, including the corneal stroma and corneal endothelium, ciliary body, and the trabecular meshwork.[6,7] Aberrant NCC development and distributions are underlying factors in ASD, a common manifestation of ARS.[8] A recent study investigated the relationship between primary cilia and anterior segment development in NCCs and revealed that the absence of primary cilia in NCCs led to ASD conditions, including abnormal corneal dimensions, defective iridocorneal angle, corneal neovascularization, disrupted Hedgehog signaling, reduced proliferation in the POM, and decreased expression of *Foxc1* and *Pitx2*.[9]

Primary cilia, microtubule-based sensory organelles projecting from cell surfaces, are indispensable for development and cellular homeostasis. They regulate Hedgehog, Notch and Wnt signaling pathways.[10,11] Mutations in ciliary protein-encoding genes cause ciliopathies, developmental disorders affecting various organs.[12–14] Intraflagellar transport (IFT) assembles and maintains primary cilia through retrograde IFT-A and anterograde IFT-B components.[15,16] IFT46, a crucial component of the IFT-B core complex, plays a pivotal role in cilia assembly and the establishment of

a stable IFT-B core complex through its interaction with IFT52.[17]

Global mutant mice for *Ift46* were embryonic lethal at E10.5 and exhibited neural tube defect, cardiac edema, and randomized heart looping because of the lack of primary cilia,[18] limiting functional studies during ocular development. This study explores the functional significance of the primary cilia-related gene *Ift46* in NCCs and its role in anterior segment development. We demonstrate that the NC-specific deletion of *Ift46* (NC-*Ift46* $^{F/F}$) results in a spectrum of ASD abnormalities, including corneal thickening, irregular iris morphology, lens-corneal attachment, defective corneal endothelium, lens epithelial invasion into the corneal stroma, and the development of corneal neovascularization. Notably, the NC-specific deletion of *Ift46* leads to increased cell proliferation in the corneal stroma, along with elevated expression of key transcriptional regulators for anterior segment development, namely Foxc1, Foxc2, and Pitx2, which are normally expressed in NCCs. Additionally, we observed decreased Sonic Hedgehog (Shh) signaling in the POM and increased Notch signaling in the corneal stroma. These findings underscore the essential role of primary cilia in NCCs for proper anterior segment formation and the establishment of corneal avascularity during early ocular development.

Methods

Animals

Conditional *Ift46*$^{F/F}$ mice[19] and *Wnt1-Cre2* mice were used in the experiments. *Wnt1-Cre2;Ift46*$^{F/F}$ (NC-*Ift46*$^{F/F}$) mice were generated by crossing *Ift46*$^{F/F}$ mice with *Wnt1-Cre2;Ift46*$^{F/+}$ mice. *Wnt1-Cre2, KRT14-Cre, Gli1*^{lacZ}, *CBF:H2B-Venus*, and *ROSA*^{mTmG} mice were purchased from Jackson Laboratory (Bar Harbor, ME, USA). For cell fate mapping of NCCs, *Wnt1-Cre2;Ift46*$^{F/+}$ mice were crossed with *Ift46*$^{F/F}$ carrying the cell membrane-targeted *ROSA*^{mTmG} reporter. *Gli1*^{lacZ} and *CBF:H2B-Venus* reporters were used to assess Shh and Notch signal activities, respectively. For corneal epithelial fate mapping, *KRT14-Cre;Ift46*$^{F/+}$*;ROSA26* and *KRT14-Cre;Ift46*$^{F/F}$*;ROSA26* mice were generated by crossing *KRT14-Cre;Ift46*$^{F/+}$ mice with *Ift46*$^{F/F}$*;ROSA26* mice. Genomic DNA from yolk sacs or tails by proteinase K treatment underwent PCR for DNA genotyping. Embryonic age was determined, with noon on the day of the vaginal plug designated as embryonic day 0.5 (E0.5). All experimental procedures complied with the ARVO Statement for the Use of Animals in Ophthalmic and Vision Research, and the experimental protocols used in this study were approved by the Institutional Animal Care and Use Committee of Ewha Womans University.

Picro-Sirius Red Staining

Picro-sirius red staining facilitates the differentiation of collagen fibers (red) from other muscle fibers and cytoplasm (yellow). Paraffin sections of eyes at E15.5 and E17.5 underwent a staining process using Picro-Sirius Red Solution (Abcam, Cambridge, MA, USA). The sections were stained for 60 minutes, followed by a rapid rinse in two changes of a 0.5% acetic acid solution. Subsequently, they were rinsed in 100% ethanol, dehydrated in two changes of 100% ethanol, and mounted with CC/Mount (Sigma-Aldrich Corp., St. Louis, MO, USA).

Corneal Flat Mounting

Corneal flat mounting was performed following established procedures as described in a previous publication.[20] In brief, enucleated eyes were fixed in 4% paraformaldehyde (PFA) for 20 minutes at 4°C, briefly rinsed in PBS, and halved. The removal of the lens, retina, and lens-encasing blood vessels was performed in 0.3% BSA/PBS, and the corneas were radially cut for ease of mounting. The corneas were then immersed in ice-cold 100% methanol for 30 minutes, permeabilized in 1% Triton X-100/PBS for 20 minutes at 4°C, and subsequently stained with CD31 and Lyve-1 antibodies to visualize blood and lymphatic vessels, respectively.

Immunohistochemical Analyses

Embryos and tissues were fixed in 4% PFA/PBS for two hours at 4°C, dehydrated, cleared in xylene, embedded in paraffin, and sectioned into 8-µm slices. Deparaffinized sections underwent hematoxylin and eosin staining and/or immunohistochemical analyses. For antigen retrieval, sections were boiled in citrate buffer (pH 6.0; Abcam), unmasked on a hot plate for 30 minutes, and washed in PBS. For 3,3′-diaminobenzidine stain, endogenous peroxidase activity was blocked with 3% hydrogen peroxide for 10 minutes, and nonspecific binding was blocked with the Protein Block (Abcam) for five minutes.

For frozen section, PFA-fixed ocular tissues were equilibrated in 10% sucrose/PBS for 20 minutes at 4°C to prevent excessive shrinkage of the anterior segment and the attachment of the lens and cornea. They were then embedded in frozen section compound (Leica, Wetzlar, Germany) and sectioned (8 µm thick) for immunostaining.

Sections were incubated with appropriate primary antibodies in a blocking solution at 4°C overnight, washed in 0.05% Tween 20/PBS four times for five minutes each to eliminate nonspecific binding, incubated with secondary antibodies at RT for two hours, counterstained with DAPI, and mounted with Vectashield (Vector Laboratories, Burlingame, CA, USA). The primary antibodies used included mouse anti-N-cadherin (clone 13A9, 1:100; Upstate Biotechnology, Charlottesville, VA, USA), mouse anti-α smooth muscle actin FITC conjugated (1:500; Sigma-Aldrich Corp.), goat anti-mouse LYVE1 (1:100; R&D systems, Minneapolis, MN, USA), PE-conjugated anti-mouse CD31 (PECAM-1, 1:200; BD Pharmingen), rabbit anti-Cyclin D1 (1:100; Abcam), rabbit anti-FOXC1 (1:100; Abcam), sheep anti-mouse FoxC2 (1:100; R&D systems), sheep anti-hPITX2 (1:100; R&D systems), rabbit anti-PAX6 (1:100; Abcam), mouse anti-cytokeratin 14 (1:100, Abcam), and rabbit anti-ARL13B (1:100; Proteintech, Rosemont, IL, USA). Secondary antibodies were Alexa Fluor 488 donkey anti-goat IgG, Alexa Fluor 594 donkey anti-mouse IgG, Alexa Fluor 594 donkey anti-rabbit IgG, and Alexa Fluor 594 donkey anti-sheep IgG (all from Invitrogen, Carlsbad, CA, USA).

X-Gal Staining

GLI1 expression and the cell fate mapping of epithelial cells were determined through X-gal staining in mice carrying a GLI1-LacZ reporter or an epithelial cell-specific ROSA26-conditional LacZ reporter, respectively. X-gal staining was performed following established procedures, as described in a previous publication.[20]

Investigative Ophthalmology & Visual Science

Transmission Electron Microscopy

Eyes at E17.5 were fixed in a solution of fresh, ice-cold 2% glutaraldehyde/2% paraformaldehyde in 0.1 M PBS (pH 7.4) overnight at 4°C and subsequently washed three times for 30 minutes in 0.1 M PBS (pH 7.4). After fixation, the eyes were post-fixed with 1% osmium tetroxide (OsO4) for two hours, washed in 0.1 M PBS (pH 7.4) for two hours, dehydrated in a graded ethanol series, and incubated with propylene oxide before embedding in a Poly/Bed 812 kit (Polysciences, Warrington, PA, USA). After being embedded in pure fresh resin, the samples were placed in an electron microscope oven (TD-700; DOSAKA, Kyoto, Japan) at 60°C for 24 hours. Ultrathin sections (80 nm) were cut from the polymer using a Leica Ultracut UCT Ultramicrotome (Leica Microsystems, Wetzlar, Germany). These sections were mounted on copper grids and stained for 20 minutes with 7% uranyl acetate and lead citrate for contrast. Imaging was conducted using a JEM-1011 electronic microscope (JEOL, Tokyo, Japan).

Statistical Analysis

Statistical comparisons between groups were evaluated with the Student *t*-test. Data are presented as mean ± SEM. $P < 0.05$ was considered significant.

Results

Ift46 in NCCs Is Required for the Ocular Anterior Segment Development

During early eye development, NCCs contribute to the formation of the ocular anterior segment. To investigate the cell type-specific functions of Ift46 during ocular development, mice with an NC-specific deletion of *Ift46* (NC-*Ift46*$^{F/F}$) were generated by crossing *Ift46*^{F} mice with *Wnt1-Cre2* mice. NC-*Ift46* $^{F/F}$ mice exhibited a spectrum of ocular anomalies, including smaller eyes with disrupted irises, and irregularly shaped smaller pupils (Figs. 1A, 1B). Histological analysis revealed multiple abnormalities in the anterior segment of NC-*Ift46*$^{F/F}$ mice, including hypoplasia of the anterior chamber, abnormal corneal thickening, irregular retinal breaks, infiltration of mesenchymal cells into the vitreous chamber, and the invasion of lens epithelium to the corneal stroma (Figs. 1C, 1D). We further investigated whether the conditional deletion of *Ift46* in corneal epithelial cells from the surface ectoderm, apart from NCCs, influenced anterior segment development. Notably, in the case of epithelium-specific *Ift46*$^{F/F}$ (*KRT14-Ift46*$^{F/F}$) mice, we observed unaltered anterior segment development, including the normal migration into the corneal epithelium (Supplementary Figs. S1A, S1B). These findings underscore the critical role of primary cilia in NCCs for the proper development of the anterior segment.

Collagen matrix accumulation in NC-*Ift46*$^{F/F}$ mice at E15.5 and E17.5 exhibited a significant impairment (Fig. 1E). Ultrastructural examination of the corneal stroma in NC-*Ift46*$^{F/F}$ mice at E17.5 revealed an irregularly shaped and disorganized stromal structure, characterized by collagen fibers deposited in swirling patterns, as opposed to the orderly alignment of collagen fibers observed in *Ift46*$^{F/F}$ mice. This anomalous collagen fibrillar arrangement resulted in severe damage to the corneal stroma in NC-*Ift46*$^{F/F}$ mice (Fig. 1F). Moreover, NC-*Ift46*$^{F/F}$ mice exhibited a failure in corneal endothelial formation, as evidenced by the absence of N-cadherin positive corneal endothelial cells (Fig. 1G). These findings unequivocally demonstrate the indispensable role of *Ift46* in the development of the ocular anterior segment, particularly in processes dependent on NCCs.

NC-Specific Deletion of Ift46 Does Not Alter the Corneal Epithelial Identity but Leads to the Invasion of Lens Epithelium and Extraocular Muscles Into the Corneal Stroma

The corneal epithelium, crucial in early ocular development, originates from the surface ectoderm and interacts closely with the NC-derived corneal stroma. Maintenance of corneal epithelial identity involves the key regulator paired box 6 (PAX6).[21] To investigate whether *Ift46* deficiency in NCCs affects with corneal epithelial identity and maintenance, we analyzed the expression of ocular epithelial markers PAX6 and cytokeratin 14 (K14) in *Ift46*$^{F/F}$ and NC-*Ift46*$^{F/F}$ mice at E15.5. PAX6 and K14 expression remained unaltered in the corneal epithelium, indicating preserved epithelial identity. However, in NC-*Ift46*$^{F/F}$ mice, we observed PAX6-positive cells in the corneal stroma, suggesting lens epithelium infiltration (Fig. 2A). Additionally, smooth muscle actin–positive extraocular muscles invaded the corneal stroma at E15.5 and E17.5 (Fig. 2B). These findings suggest that the compromised corneal endothelial barrier and stromal disruptions create conditions facilitating lens epithelium and extraocular muscle invasion into the corneal stroma.

NC-Specific Deletion of *Ift46* Does Not Alter the Migration of NCCs but Leads to the Loss of Primary Cilia in NCCs

To investigate the impact of *Ift46* deletion in NCCs on their migration to the periocular and corneal mesenchyme during the critical period of anterior segment development from E11.5 to E16.5, we analyzed NCC migration using the *ROSA*^{mTmG} *(mT/mG)* conditional Cre reporter, allowing for Cre-dependent mG labeling.[22] Subsequently, we examined the fate of Cre-expressing NCCs. Our observations indicated that NCCs in NC-*Ift46*$^{F/F}$ mice exhibited normal migration to the periocular and corneal mesenchyme, as well as hyaloid vessels of NC origin during the designated timeframe, aligning with findings in NC-*Ift46*$^{F/+}$*;mT/mG* mice. An intriguing observation was the ectopic invasion of lens epithelium into the cornea in NC-*Ift46*$^{F/F}$ mice at E13.5. Importantly, these invading cells were not of NC origin, as evidenced by the absence of Cre-dependent mG labeling at both E13.5 and E16.5 (Fig. 3A).

Given its crucial role in primary cilia assembly, *Ift46* deficiency results in the loss of these vital organelles. To validate the specific deletion of *Ift46* in NCCs within ocular mesenchyme, we conducted immunostaining to assess the presence of primary cilia in NCCs. This involved analyzing the ocular mesenchyme of NC-*Ift46*$^{F/+}$*;mT/mG* and NC-*Ift46*$^{F/F}$*;mT/mG* mice, using the cilia marker Arl13b to identify cilia in NCCs. At E13.5, NC-*Ift46*$^{F/+}$*;mT/mG* mice exhibited cilia presence in the ocular mesenchyme and epithelium, independent of mG labeling. In contrast, in NC-*Ift46*$^{F/F}$*;mT/mG* mice, cilia were notably absent in the mG-labeled ocular mesenchyme of NC origin, while they remained intact in the mT-labeled epithelium originating from the neuroectoderm (Fig. 3B). These findings

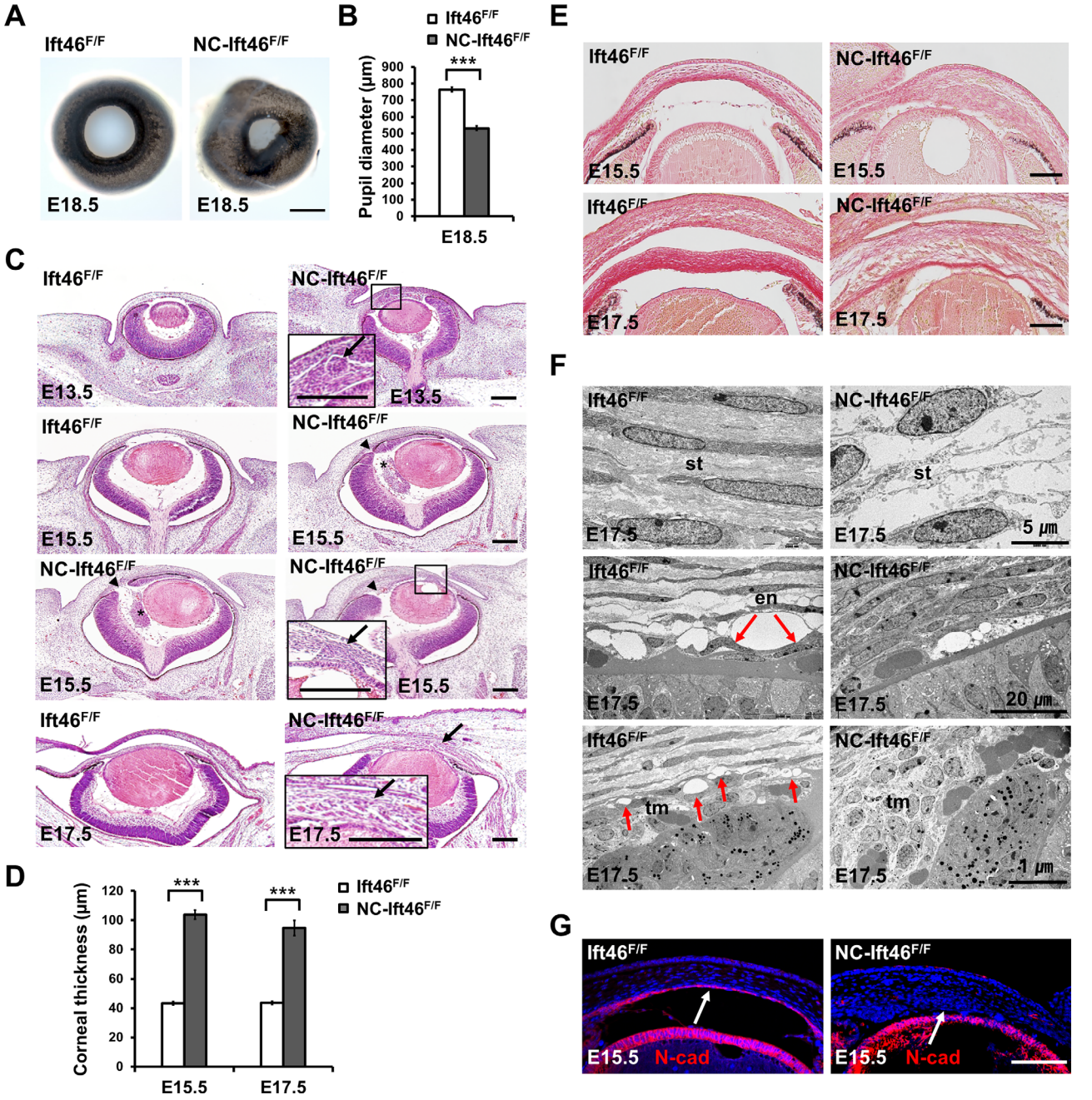

Figure 1. NC-specific deletion of *Ift46* leads to anterior segment dysgenesis. (**A**) Comparison of eyeballs from *Ift46*$^{F/F}$ and NC-*Ift46*$^{F/F}$ mice at E18.5. NC-*Ift46*$^{F/F}$ mice displayed irregularities in the iris and pupil. (**B**) Quantification of pupil diameter in *Ift46*$^{F/F}$ and NC-*Ift46*$^{F/F}$ mice at E18.5. (**C**) Hematoxylin & eosin staining of eyes from *Ift46*$^{F/F}$ and NC-*Ift46*$^{F/F}$ mice at E13.5 and E15.5. NC-*Ift46*$^{F/F}$ mice displayed multiple anterior segment defects, including thickened corneal stroma, hypoplastic anterior chamber, displaced pupil, abnormal tissue infiltration in the corneal stroma (**inset**, *arrows*), and retinal breaks (*arrowheads*) with aberrant tissue detachment (*asterisks*) into the vitreous chamber. (**D**) Quantification of corneal thickness in *Ift46*$^{F/F}$ and NC-*Ift46*$^{F/F}$ mice at E15.5 and E17.5. (**E**) Impaired collagen formation in the corneal stroma of NC-*Ift46*$^{F/F}$ mice. Picro-sirius staining revealed reduced collagen formation (*pinkish-red*) in the corneal stroma of NC-*Ift46*$^{F/F}$ mice at E15.5 and E17.5. (**F**) Transmission electron microscopy images illustrating the ultrastructure of corneal stroma, endothelium, and trabecular meshwork at E17.5. NC-*Ift46*$^{F/F}$ mice displayed disorganized collagen fibers in the corneal stroma (*upper panel*), the lack of corneal endothelium (*middle panel*), and abnormal trabecular meshwork (*bottom panel*). (**G**) Lack of corneal endothelium in NC-*Ift46*$^{F/F}$ mice. Immunostaining of the corneal endothelium marker N-cadherin revealed the absence of corneal endothelium (*arrow*) in NC-*Ift46*$^{F/F}$ mice at E15.5. en, endothelium; st, stroma; tm, trabecular meshwork. *Scale bars*: 500 μm in A; 100 μm in C, E and G. ***$P < 0.001$, Student's *t*-test.

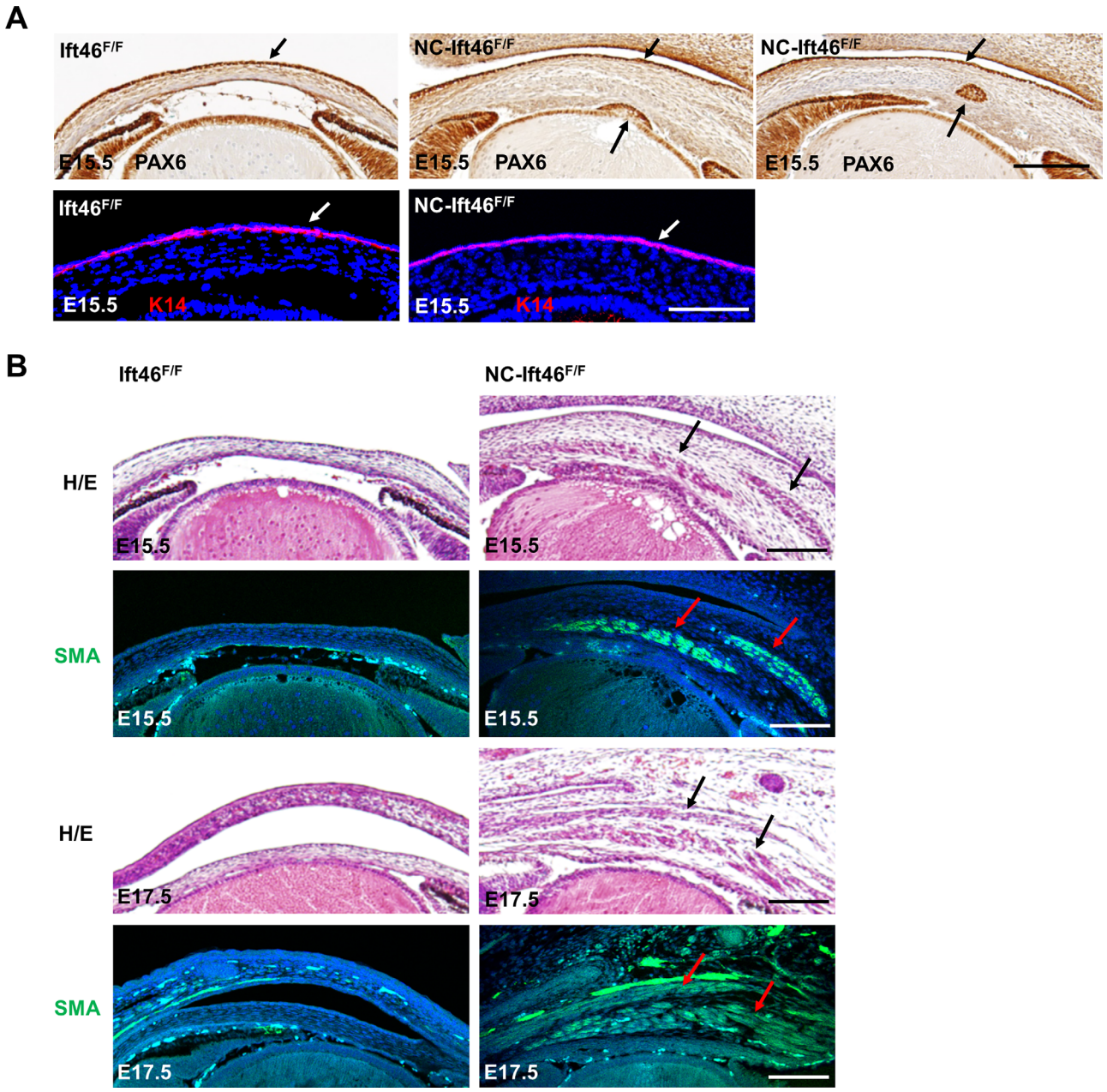

Figure 2. NC-specific deletion of *Ift46* maintains corneal epithelial identity but leads to ectopic tissue invasion in the corneal stroma of NC-*Ift46*$^{F/F}$ mice. (**A**) The expression of ocular epithelial markers PAX6 and cytokeratin 14 (K14) in the corneas of *Ift46*$^{F/F}$ and NC-*Ift46*$^{F/F}$ mice at E15.5. NC-*Ift46*$^{F/F}$ mice exhibited the maintenance of corneal epithelial identity (*small arrows*) but displayed the invasion of the lens epithelial cells into the corneal stroma (*arrows*). (**B**) Hematoxylin & eosin staining and the expression of smooth muscle alpha actin (SMA) in the corneas of *Ift46*$^{F/F}$ and NC-*Ift46*$^{F/F}$ mice at E15.5 and E17.5. Notably, there was invasion of SMA-positive extraocular muscles (*red arrows*) into the corneal stroma of NC-*Ift46*$^{F/F}$ mice. *Scale bars*: 100 µm.

collectively confirm that the loss of primary cilia in NCCs does not hinder their migration to the ocular mesenchyme.

NC-Specific Deletion of *Ift46* Leads to Alteration of Shh Activity in the POM, Persistent Ocular Transcription Factors, and Hyperproliferation in the Corneal Mesenchyme

The primary cilium plays a crucial role in the Shh signaling pathway, which regulates cell proliferation and differentiation in developmental processes. Shh signaling primarily influences the adhesion and migration of NCCs rather than their specification.[23,24] The expression of Gli1 serves as a sensitive marker reflecting Shh signaling activity.[25] To investigate whether the absence of primary cilia affects Shh activity within the periocular and corneal mesenchyme derived from NCCs, we analyzed Shh signaling using the Gli1-LacZ reporter. At both E12.5 and E13, we observed significantly reduced Shh activity in the POM of NC-*Ift46*$^{F/F}$;*Gli1*$^{lacZ/+}$ mice compared to *Ift46*$^{F/F}$;*Gli1*$^{lacZ/+}$ mice (Fig. 4A). Notably, no Shh activity was detected in the corneal mesenchyme of

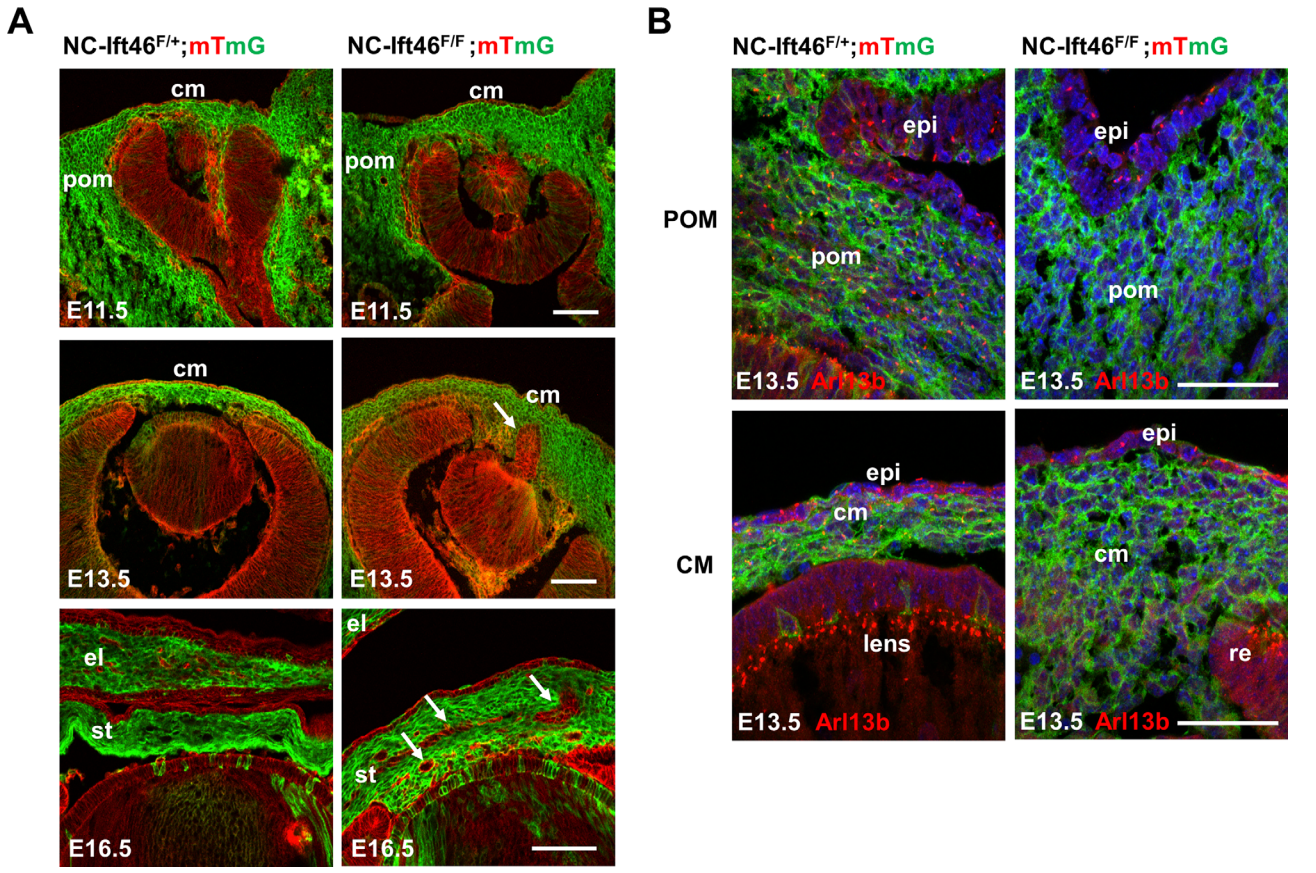

Figure 3. NC-specific deletion of *Ift46* does not alter the migration of NCCs and leads to the loss of primary cilia in the periocular and corneal mesenchyme. (**A**) Cell fate mapping of NCCs in NC-*Ift46*$^{F/+}$ and NC-*Ift46*$^{F/F}$ mice using the mTmG reporter. NCCs express the mG reporter (*green*), whereas non-NCCs express the mT reporter (*red*). Despite NC-specific Ift46 deficiency, there is no discernible alteration in the migration of NCCs to periocular mesenchyme, corneal mesenchyme, and corneal stroma during ocular development. Notably, mT-positive cells and tissues originating from non-NC sources (*arrows*) were observed within the mG-positive corneal mesenchyme and corneal stroma of NC-*Ift46*$^{F/F}$ mice at E13.5 and E16.5, in contrast to *Ift46*$^{F/F}$ mice. The presence of the lens stalk (*arrow*) is also noteworthy in NC-*Ift46*$^{F/F}$ mice at E13.5. (**B**) Loss of primary cilia in the periocular and corneal mesenchyme of NC-*Ift46*$^{F/F}$ mice. Primary cilia were stained with a cilium marker Arl13b antibody (*red arrows*). Primary cilia remained intact in NC-*Ift46*$^{F/+}$ mice but lacked in NC-*Ift46*$^{F/F}$ mice at E13.5. Note that the primary cilia in the epithelial cells of non-NC origin remained unaffected. cm, corneal mesenchyme; el, eyelid; epi, epithelium; pom, periocular mesenchyme; re, retinal epithelium; st, stroma. *Scale bars*: 100 µm.

either *Ift46*$^{F/F}$;*Gli1*$^{lacZ/+}$ or NC-*Ift46*$^{F/F}$;*Gli1*$^{lacZ/+}$ mice. These findings strongly indicate that the loss of primary cilia due to *Ift46* deficiency in NCCs has a more pronounced effect on Shh activity within the POM than in the corneal mesenchyme.

In humans, mutations of *FOXC1* and *PITX2* genes are linked to ASD, a condition characterized by anomalies in the anterior segment.[1–3] Studies in mice revealed that NC-specific deletion of *Foxc1* and compound deletion of *Foxc1* and *Foxc2* in NCCs mimic ASD conditions.[20,26,27] Our investigation showed that the ocular features of NC-*Ift46*$^{F/F}$ mice closely resemble those observed in mice with NC-specific *Foxc1* deletion. To assess how the absence of primary cilia, due to *Ift46* deficiency in NCCs, affects key ocular transcription factors, we examined Foxc1, Foxc2, and Pitx2 expression. These transcription factors predominantly originate from the periocular mesenchyme of NC origin, playing a pivotal role in anterior segment formation.[6] In NC-*Ift46*$^{F/F}$ mice, Foxc1 and Foxc2 expression persisted in the cornea mesenchyme, contrasting with the decreasing expression observed in *Ift46*$^{F/F}$ mice by E13.5. Conversely, Pitx2 expression in the corneal mesenchyme of NC-*Ift46*$^{F/F}$ mice remained unaltered (Fig. 4B), maintaining the expression pattern of Pitx2 in developing corneas.[28] The prolonged expression of ocular transcription factors in NCCs suggests sufficient migration to the eye, maintaining an abundant population during corneal development. Despite normal NCC migration, NC-*Ift46*$^{F/F}$ mice exhibited abnormal corneal thickening.

Given reduced Shh activity in the POM and persistent ocular transcription factor expression in the corneal mesenchyme of NC-*Ift46*$^{F/F}$ mice, we explored whether the loss of primary cilia in NCCs influences cell proliferation using the marker Cyclin D1. NC-*Ift46*$^{F/F}$ mice showed hyperproliferation, especially in the corneal stroma, compared to *Ift46*$^{F/F}$ mice (Figs. 4C, 4D). These findings suggest that corneal hyperproliferation in NC-*Ift46*$^{F/F}$ mice directly results from the loss of primary cilia.

NC-Specific Deletion of *Ift46* Results in Corneal Neovascularization

The cornea is typically avascular, a critical characteristic for maintaining transparency achieved through a delicate balance between proangiogenic and antiangiogenic

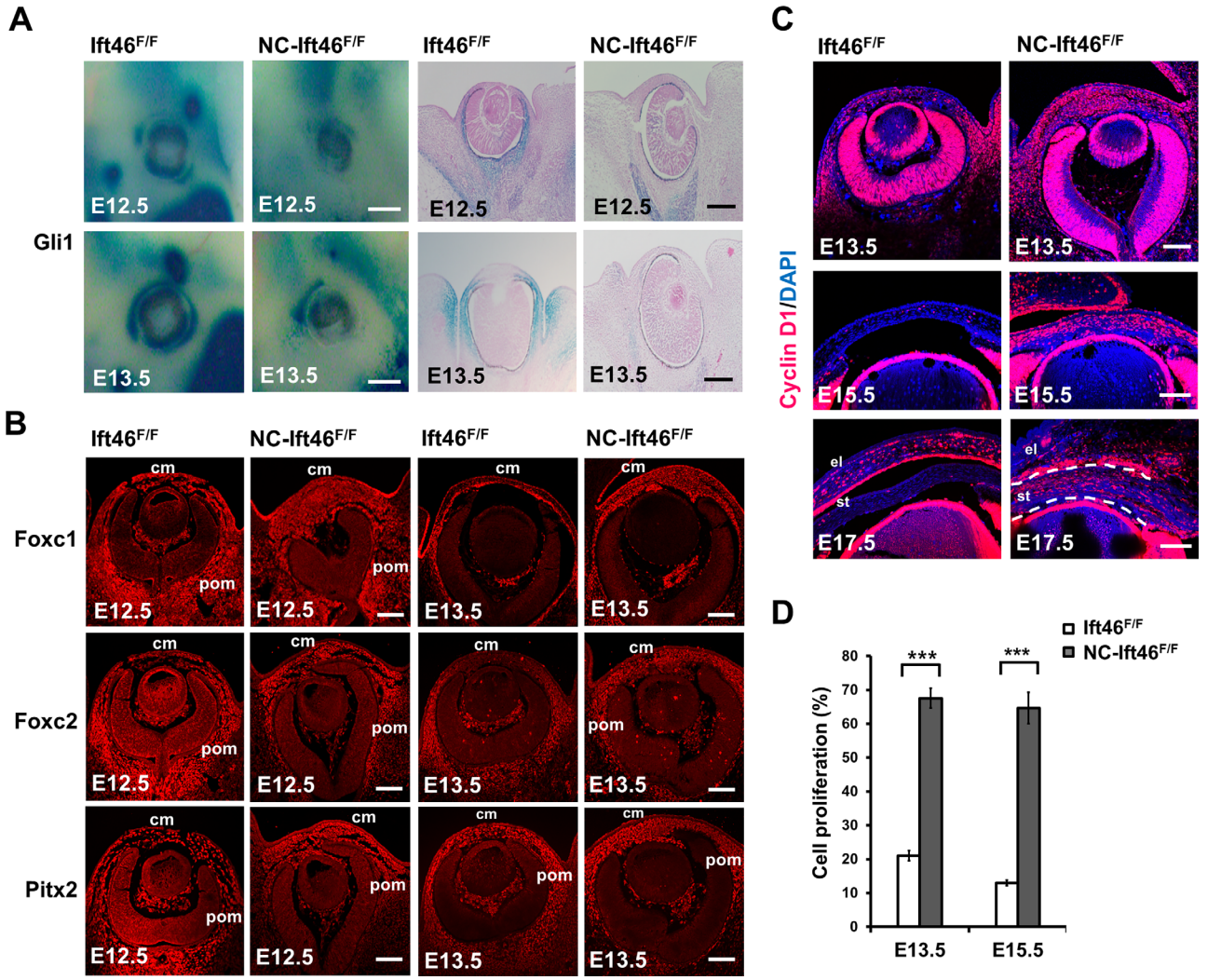

Figure 4. Loss of primary cilia by *Ift46* deficiency in NCCs induces the decrease of Shh signal activity, the increase of cell proliferation, and the persistent expression of Foxc1 and Foxc2 in the corneal mesenchyme. (**A**) Decrease of Shh signal activity in the periocular mesenchyme (POM) of NC-*Ift46*$^{F/F}$;*Gli1*$^{lacZ/+}$ mice. Shh activity was assessed by Gli1-LacZ expression in the POM of *Ift46*$^{F/F}$;*Gli1*$^{lacZ/+}$ and NC-*Ift46*$^{F/F}$;*Gli1*$^{lacZ/+}$ mice at E12.5 and E13.5. *Ift46*$^{F/F}$;*Gli1*$^{lacZ/+}$ mice displayed Gli1-LacZ expression in the POM, whereas NC-*Ift46*$^{F/F}$;*Gli1*$^{lacZ/+}$ mice exhibited a significant reduction in Gli1-LacZ expression in the POM, indicating a decrease in Shh signal activity. (**B**) Persistent expression of ocular NCC markers Foxc1 and Foxc2 in the corneal mesenchyme of NC-*Ift46*$^{F/F}$ mice at E12.5 and E13.5. The corneas from *Ift46*$^{F/F}$ and NC-*Ift46*$^{F/F}$ mice were stained with Foxc1, Foxc2, and Pitx2 antibodies. At E12.5, both *Ift46*$^{F/F}$ and NC-*Ift46*$^{F/F}$ mice displayed Foxc1 and Foxc2 expression in the POM and corneal mesenchyme. By E13.5, expression was restricted to the POM in *Ift46*$^{F/F}$ mice, whereas in NC-*Ift46*$^{F/F}$ mice, Foxc1 and Foxc2 were ectopically expressed in increased amounts in the corneal mesenchyme. Pitx2 expression remained consistent in both the periocular and corneal mesenchyme. (**C**) Hyperproliferation in the corneal stroma in NC-*Ift46*$^{F/F}$ mice. Cell proliferation in the corneal stroma of *Ift46*$^{F/F}$ and NC-*Ift46*$^{F/F}$ mice at E13.5, E15.5 and E17.5 was examined using Cyclin D1 staining. Persistent cell proliferation was observed in the corneal stroma of NC-*Ift46*$^{F/F}$ mice throughout ocular development. (**D**) Quantification of cell proliferation in the corneal stroma of *Ift46*$^{F/F}$ and NC-*Ift46*$^{F/F}$ mice at E13.5 and E15.5 through Cyclin D1 staining. cm, corneal mesenchyme; pom, periocular mesenchyme. ***$P < 0.001$, Student's *t*-test. *Scale bars*: 100 µm.

factors.[27] Studies involving temporal conditional knockout of *Pitx2* and the NC-specific deletion of *Foxc1* in mice have unveiled corneal developmental anomalies, culminating in pathological neovascularization and emphasizing their role in establishing angiogenic privilege.[20,28] This neovascularization is marked by the infiltration of blood vessels from the limbus into the corneal stroma. Given the observed ASD phenotypes and corneal neovascularization in *Foxc1* and *Pitx2* mutant mice, we investigated whether *Ift46* deficiency similarly leads to corneal neovascularization. A visual examination at E15.5 revealed ectopic blood vessels in the eyes of NC-*Ift46*$^{F/F}$ mice (Fig. 5A). To further confirm abnormal neovascularization in NC-*Ift46*$^{F/F}$ mice, we performed immunostaining for the endothelial-specific marker CD31 on corneas at E15.5 and utilized transmission electron microscopy at E17.5. This analysis confirmed the presence of ectopic blood vessels in the disrupted corneal stroma of NC-*Ift46*$^{F/F}$ mice, indicating pathological corneal neovascularization during ocular development (Fig. 5A). To identify the source of this corneal neovascularization, we conducted corneal flat mount immunostaining for CD31 at E16.5 and E18.5, as well as Lyve-1 at E18.5 in the eyes. Our analyses revealed that NC-*Ift46*$^{F/F}$ mice exhibited ectopic outgrowths of CD31-positive blood vessels orig-

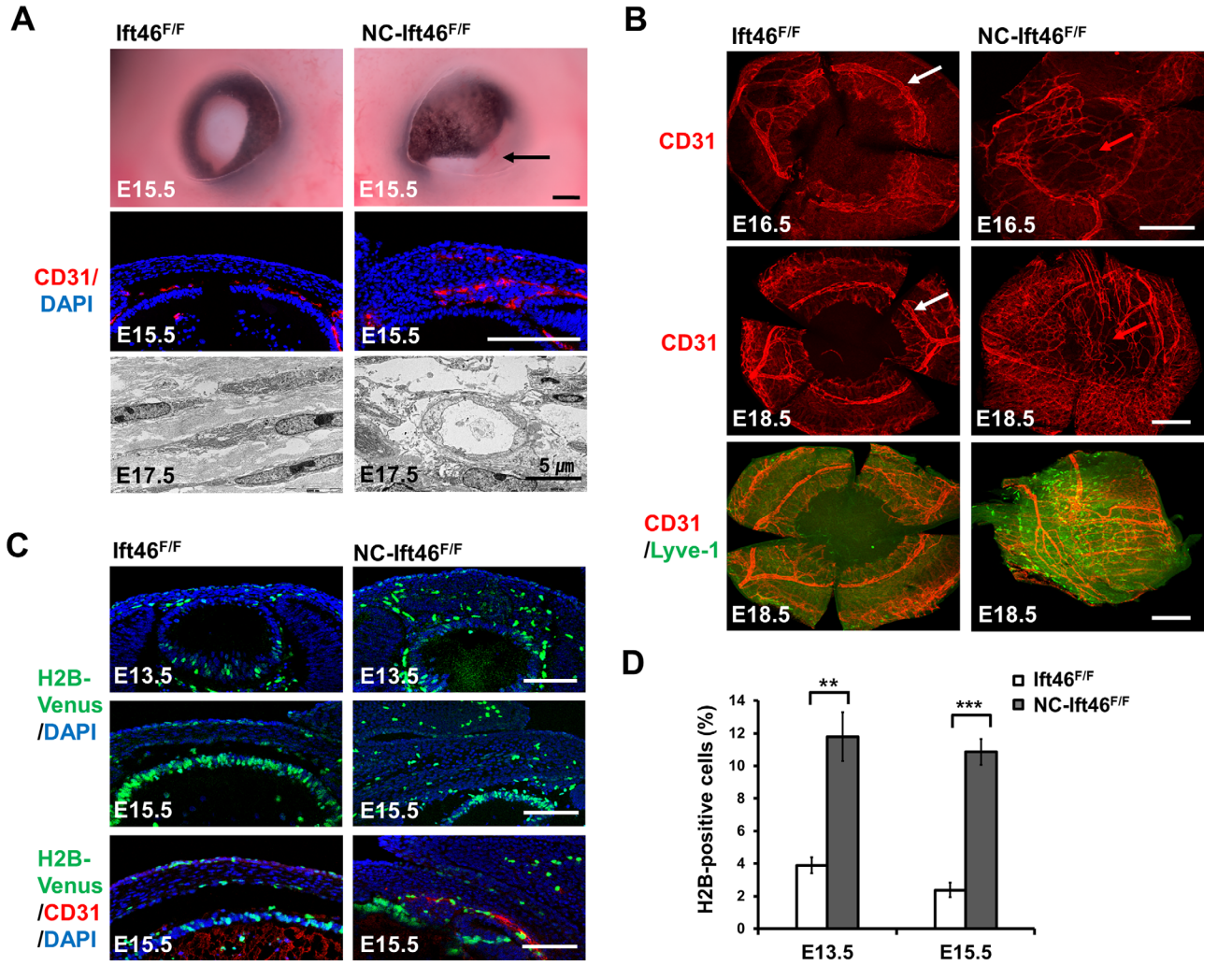

Figure 5. NC-specific deletion of *Ift46* induces corneal neovascularization and increase of Notch activity. (**A**) Neovascularization in the corneal stroma of NC-*Ift46*$^{F/F}$ mice at E15.5 and E17.5. Neovascularization (*arrow*) in the eye of NC-*Ift46*$^{F/F}$ mice at E15.5 was observed through light microscopy (*upper panel*). Immunostaining of vascular endothelial-specific marker CD31 (*middle panel*) at E15.5 and transmission electron microscopy (TEM) (*bottom panel*) at E17.5 confirmed neovascularization of the corneal stroma in NC-*Ift46*$^{F/F}$ mice. (**B**) Corneal flat mount immunostaining of *Ift46*$^{F/F}$ and NC-*Ift46*$^{F/F}$ mice at E16.5 and E18.5. Corneal neovascularization was examined by vascular endothelial-specific marker CD31 staining (*upper* and *middle panels*). While *Ift46*$^{F/F}$ mice displayed avascular corneas with well-defined limbal blood vessels (*white arrows*), NC-*Ift46*$^{F/F}$ mice exhibited extensive vascularization (*red arrows*) with disrupted limbal blood vessels. Lymphangiogenesis was examined by the lymphatic vessel marker Lyve-1 staining at E18.5 (*bottom panel*). The cornea of *Ift46*$^{F/F}$ mice remained Lyve-1 negatives, whereas the cornea of NC-*Ift46*$^{F/F}$ mice showed remarkable infiltration of Lyve-1 positive cells (*green*). (**C**) Increase of Notch signaling activity in the corneal stroma of NC-*Ift46*$^{F/F}$ mice. Elevated Notch signaling activity was observed in the corneas of NC-*Ift46*$^{F/F}$ mice, as evidenced by the examination of *H2B-Venus* reporter expression in the corneas at E13.5 and E15.5 (*upper* and *middle panels*), with subsequent colocalization with CD31 (*bottom panel*) at E15.5, indicating an augmented Notch signaling response in the corneal stroma of NC-*Ift46*$^{F/F}$ mice. (**D**) Quantification of *H2B-Venous* positive cells in the corneal stroma of *Ift46*$^{F/F}$ and NC-*Ift46*$^{F/F}$ mice at E13.5 and E15.5. $^{**}P < 0.01$, $^{***}P < 0.001$, Student's *t*-test. *Scale bars*: 100 µm.

inating from the limbus, accompanied by scattered Lyve-1-positive macrophages throughout the entire cornea. This was associated with a complete disruption of the vascular architecture when compared to the eyes of *Ift46*$^{F/F}$ mice, which displayed an avascular cornea with a well-organized vascular limbus (Fig. 5B). These findings strongly suggest that primary cilia play a crucial role in establishing an angiogenic privilege for the avascular cornea.

After observing hyperproliferation and neovascularization in the corneal stroma of NC-*Ift46*$^{F/F}$ mice, we investigated the involvement of Notch signaling in this process using the *H2B-Venus* reporter, renowned for tracing Notch expression within the vasculature and epithelium.[29] Our findings revealed a significant ectopic increase in Notch signaling activity within the corneal stroma of NC-*Ift46*$^{F/F}$ mice, as evidenced by *H2B-Venus* expression, without any discernible impact on the epithelial layer (Figs. 5C, 5D). Particularly noteworthy was the observed colocalization of *H2B-Venus* with CD31-positive vascular cells in the corneal stroma of NC-*Ift46*$^{F/F}$ mice (Fig. 5C). This alignment coincided with the outgrowth of CD31-positive blood vessels at E15.5, as demonstrated by the overlapping presence of CD31-positive cells and *H2B-Venus*-expressing cells. Collectively, these findings underscore the pivotal role of primary cilia in NCCs in preserving corneal avascularity.

Discussion

Our findings highlight the crucial role of primary cilia in anterior segment development, originating primarily from NCCs. Deletion of *Ift46* in NCCs leads to the loss of primary cilia, resulting in ASD-associated phenotypes. These include corneal thickening, collagen matrix disorganization, anterior chamber hypoplasia, trabecular meshwork disruption, and neovascularization, closely associated with alterations in Shh and Notch signaling.

Moreover, key genes regulating ocular development, such as *Foxc1* and *Foxc2*, persistently express in the corneal mesenchyme of NC-*Ift46*$^{F/F}$ mice. This contributes to ASD manifestations affecting the cornea, iris, and trabecular meshwork.[1,2] Critical genes associated with ASD in humans, including *FOXC1, PITX2* and *PAX6,* exhibit various phenotypes because of genetic variants.[3–5,30] Mutations in *FOXC1* and *PITX2* in human patients with ARS are linked to pathological corneal neovascularization.[20,31]

NCCs play a pivotal role in anterior segment development. Mutations in key regulators *Foxc1, Foxc2* and *Pitx2* in mice result in aberrant anterior segment structures characterized by corneal thickening and neovascularization.[20,26,28] Noteworthy is the sustained expression of these genes and increased Notch activity in the corneal mesenchyme of NC-*Ift46*$^{F/F}$ mice, contributing to observed corneal neovascularization. Additionally, the temporal conditional knockout of *Pitx2* during corneal development initiates the expansion of Foxc2 expression into the corneal mesenchyme.[28] The pathological corneal neovascularization associated with *FOXC1* duplication in certain patients with ARS [20] may elucidate expanded expression of Foxc1 and concurrent corneal neovascularization in NC-*Ift46*$^{F/F}$ mice, suggesting a significant role for primary cilia in corneal mesenchyme specification and angiogenic privilege.

The impairment of Shh signaling activity, particularly through primary cilia, is correlated with severe ocular abnormalities, emphasizing its critical role in the anterior segment formation and its association with ocular developmental disorders such as ASD.[32,33] Primary cilia, formed through IFT machinery, are essential for various cellular functions. Mutations in the components of the IFT-B complex lead to the shortening or loss of primary cilia, disrupting Shh signaling and causing ciliopathies.[17,34] The deletion of *Ift46* in NCCs results in the loss of primary cilia, which, in turn, abolishes Shh signaling activity in the POM and leads to ocular malformations.

Primary cilia play a significant role in regulating cell behavior, particularly in influencing cell cycle progression and suppressing proliferative signaling.[35–37] The disassembly of primary cilia facilitates cell proliferation, and their absence is linked to excessive cell proliferation observed in conditions like cancer.[35,36] Signaling pathways like Shh and Notch, known regulators of cell proliferation and differentiation across various tissues and cell types, are influenced by primary cilia.[23,38,39] Deletion of *Ift88* or *Kif3a* in different contexts results in hyperproliferation in the epidermis or myoblasts.[38,39] The loss of primary cilia because of *Ift46* deletion in NCCs leads to hyperproliferation in the corneal mesenchyme, associated with ASD-associated genes *Foxc1* and *Foxc2*, emphasizing the impact of ciliary functions on the control of cell proliferation. The phenotypes observed in NC-*Ift46*$^{F/F}$ mice closely resemble those in mice with mutations in *Foxc1, Foxc2* and *Pitx2*.[20,26,28] A notable distinction lies in the corneal phenotypes between NC-*Ift46*$^{F/F}$ mice and NC-*Ift88* $^{F/F}$ mice. In contrast to NC-*Ift46*$^{F/F}$ mice, NC-*Ift88*$^{F/F}$ mice exhibit a thinned cornea, partial corneal neovascularization, reduced cell proliferation in a subset of the POM, and decreased *Foxc1* and *Pitx2* expression.[9] This underscores the unique spatiotemporal expression and diverse phenotypic outcomes associated with the similar and/or different roles of ciliary genes in mediating developmental signaling in tissue-specific and stage-specific contexts.[40,41] Understanding the context-specific roles of ciliary genes and their intricate interactions with signaling pathways is essential for comprehending the multifaceted phenotypes of ciliopathies.

In conclusion, our findings highlight the essential role of the ciliary gene *Ift46* in the development of the anterior segment and the maintenance of corneal avascularity. The deletion of *Ift46* in NCCs, resulting in the loss of primary cilia, contributes to the manifestations of ASD phenotypes. Our findings provide compelling evidence for a significant association between primary cilia and the pathogenesis of ASD, implying the potential link of primary cilia to ARS.

Acknowledgments

Supported by the National Research Foundation of Korea (NRF) grants funded by the Korea government (MSIT) (Nos. 2017R1D1A1B0302889, 2020R1A3B2079811, 2022R1A2C3002899, and RS-2023-00217798).

Disclosure: **S. Seo**, Imvastech (E); **S.K. Sonn**, None; **H.Y. Kweon**, None; **J. Jin**, None; **T. Kume**, None; **J.Y. Ko**, None; **J.H. Park**, None; **G.T. Oh**, Imvastech (E)

References

1. Reis LM, Semina EV. Genetics of anterior segment dysgenesis disorders. *Curr Opin Ophthalmol.* 2011;22:314–324.
2. Kuang L, Zhang M, Wang T, et al. The molecular genetics of anterior segment dysgenesis. *Exp Eye Res.* 2023;234:109603.
3. Tümer Z, Bach-Holm D. Axenfeld–Rieger syndrome and spectrum of PITX2 and FOXC1 mutations. *Eur J Hum Genet.* 2009;17:1527–1539.
4. Seifi M, Walter MA. Axenfeld-Rieger syndrome. *Clin Genet.* 2018;93:1123–1130.
5. Michels K, Bohnsack BL. Ophthalmological manifestations of Axenfeld-Rieger Syndrome: current perspectives. *Clin Ophthalmol.* 2023;17:819–828.
6. Gage PJ, Rhoades W, Prucka SK, Hjalt T. Fate maps of neural crest and mesoderm in the mammalian eye. *Invest Ophthalmol Vis Sci.* 2005;46:4200–4208.
7. Williams AL, Bohnsack BL. The ocular neural crest: specification, migration, and then what? *Front Cell Dev Biol.* 2020;8:595896.
8. Williams AL, Bohnsack BL. Neural crest derivatives in ocular development: discerning the eye of the storm. *Birth Defects Res C Embryo Today.* 2015;105:87–95.
9. Portal C, Rompolas P, Lwigale P, Iomini C. Primary cilia deficiency in neural crest cells models anterior segment dysgenesis in mouse. *eLife.* 2019;8:e52423.
10. Goetz SC, Anderson KV. The primary cilium: a signalling centre during vertebrate development. *Nat Rev Genet.* 2010;11:331–344.
11. Wheway G, Nazlamova L, Hancock JT. Signaling through the primary cilium Front *Cell Dev Biol.* 2018;6:8.
12. Bangs F, Anderson KV. Primary cilia and mammalian Hedgehog signaling. *Cold Spring Harb Perspect Biol.* 2017;9:a028175.

13. Mitchison HM, Valente EM. Motile and non-motile cilia in human pathology: from function to phenotypes. *J Pathol*. 2017;241:294–309.
14. Dominic P, Norris DP, Grimes DT. Mouse models of ciliopathies: the state of the art. *Dis Model Mech*. 2012;5:299–312.
15. Ishikawa H, Marshall WF. Ciliogenesis: building the cell's antenna. *Nat Rev Mol Cell Biol*. 2011;12:222–234.
16. Taschner M, Lorentzen E. The intraflagellar transport machinery. *Cold Spring Harb Perspect Biol*. 2016;8:a028092.
17. Taschner M, Kotsis F, Braeuer P, Kuehn EW, Lorentzen E. Crystal structures of IFT70/52 and IFT52/46 provide insight into intraflagellar transport B core complex assembly. *J Cell Biol*. 2014;207:269–282.
18. Lee MS, Hwang KS, Oh HW, et al. IFT46 plays an essential role in cilia development. *Dev Biol*. 2015;400:248–257.
19. Lee EJ, Ko JY, Oh S, et al. Autophagy induction promotes renal cyst growth in polycystic kidney disease. *EBioMedicine*. 2020;60:102986.
20. Seo S, Singh HP, Lacal PM, et al. Forkhead box transcription factor FoxC1 preserves corneal transparency by regulating vascular growth. *Proc Natl Acad Sci*. 2012:109:2015–2020.
21. Ouyang H, Xue Y, Lin Y, et al. WNT7A and PAX6 define corneal epithelium homeostasis and pathogenesis. *Nature*. 2014;511(7509):358–361.
22. Muzumdar MD, Tasic B, Miyamichi K, Li L, Luo L. A global double-fluorescent Cre reporter mouse. *Genesis*. 2007;45:593–605.
23. Jia Y, Wang Y, Xie J. The Hedgehog pathway: role in cell differentiation, polarity and proliferation. *Arch Toxicol*. 2015;89:179–191.
24. Testaz S, Jarov A, Williams KP, et al. Sonic Hedgehog restricts adhesion and migration of neural crest cells independently of the Patched-Smoothened-Gli signaling pathway. *Proc Natl Acad Sci*. 2001;98:12521–12526.
25. Bai CB, Auerbach W, Lee J S, Stephen D, Joyner AL. Gli2, but not Gli1, is required for initial Shh signaling and ectopic activation of the Shh pathway. *Development*. 2002;129:4753–4761.
26. Seo S, Chen L, Liu W, et al. Foxc1 and Foxc2 in the neural crest are required for ocular anterior segment development. *Invest Ophthalmol Vis Sci*. 2017;58:1368–1377.
27. Ellenberg D, Azar DT, Hallak JA, et al. Novel aspects of corneal angiogenic and lymphangiogenic privilege. *Prog Retin Eye Res*. 2010;29:208–248.
28. Gage PJ, Kuang C, Zacharias AL. The homeodomain transcription factor PITX2 is required for specifying correct cell fates and establishing angiogenic privilege in the developing cornea. *Dev Dyn*. 2014;243:1391–1400.
29. Nowotschin S, Xenopoulos P, Schrode N, Hadjantonakis A-K. A bright single-cell resolution live imaging reporter of Notch signaling in the mouse. *BMC Dev Biol*. 2013;13:15.
30. Micheal S, Siddiqui SN, Zafar SN, et al. A novel homozygous mutation in FOXC1 causes Axenfeld Rieger syndrome with congenital glaucoma. *PLoS ONE*. 2016;11(7):e0160016.
31. Kletke SN, Vincent A, Maynes JT, et al. A de novo mutation in *PITX2* underlies a unique form of Axenfeld-Rieger syndrome with corneal neovascularization and extensive proliferative vitreoretinopathy. *Ophthalmic Genet*. 2020;41:358–362.
32. Burnett JB, Lupu FI, Eggenschwiler JT. Proper ciliary assembly is critical for restricting Hedgehog signaling during early eye development in mice. *Dev Biol*. 2017;430:32–40.
33. Cavodeassi F, Creuzet S, Etchevers HC. The Hedgehog pathway and ocular developmental anomalies. *Hum Genet*. 2019;138:917–936.
34. Wang W, Jack BM, Wang HH, Kavanaugh MA, Maser RL, Tran PV. Intraflagellar transport proteins as regulators of primary cilia length. *Front Cell Dev Biol*. 2021;9:661350.
35. Seeley ES, Nachury MV. The perennial organelle: assembly and disassembly of the primary cilium. *J Cell Sci*. 2010;123:511–518.
36. Basten SG, Giles RH. Functional aspects of primary cilia in signaling, cell cycle and tumorigenesis. *Cilia*. 2013;2:6.
37. Goto H, Inoko A, Inagaki M. Cell cycle progression by the repression of primary cilia formation in proliferating cells. *Cell Mol Life Sci*. 2013;70:3893–3905.
38. Ezratty E, Stokes N, Chai S, Shah A, Fuchs E. A role for the primary cilium in Notch signaling and epidermal differentiation during skin development. *Cell*. 2011;145:1129–1141.
39. Venugopal N, Ghosh A, Gala H, Aloysius A, Vyas N, Dhawan J. The primary cilium dampens proliferative signaling and represses a G2/M transcriptional network in quiescent myoblasts. *BMC Mol Cell Biol*. 2020;21:25.
40. Snedeker J, Schock EN, Struve JN, et al. Unique spatiotemporal requirements for intraflagellar transport genes during forebrain development. *Plos One*. 2017;12(3):e0173258.
41. Heydeck W, Fievet L, Davis EE, Katsanis N. The complexity of the cilium: spatiotemporal diversity of an ancient organelle. *Curr Opin Cell Biol*. 2018;55:139–149.

Investigative Ophthalmology & Visual Science